ChemComm

Accepted Manuscript

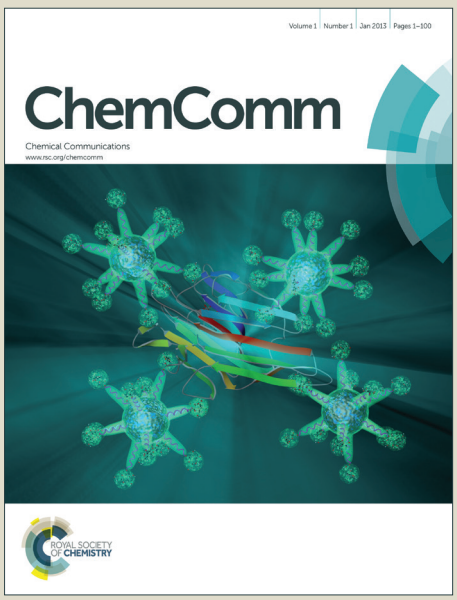

This is an *Accepted Manuscript*, which has been through the Royal Society of Chemistry peer review process and has been accepted for publication.

Accepted Manuscripts are published online shortly after acceptance, before technical editing, formatting and proof reading. Using this free service, authors can make their results available to the community, in citable form, before we publish the edited article. We will replace this *Accepted Manuscript* with the edited and formatted *Advance Article* as soon as it is available.

You can find more information about *Accepted Manuscripts* in the Information for Authors.

Please note that technical editing may introduce minor changes to the text and/or graphics, which may alter content. The journal's standard Terms & Conditions and the Ethical guidelines still apply. In no event shall the Royal Society of Chemistry be held responsible for any errors or omissions in this *Accepted Manuscript* or any consequences arising from the use of any information it contains.

ROYAL SOCIETY OF CHEMISTRY

www.rsc.org/chemcomm

Cite this: DOI: 10.1039/c0xx00000x

www.rsc.org/xxxxxx

ARTICLE TYPE

Signal-on Electrochemiluminescent Aptasensor Based on Target Controlled Permeable Films

Lichan Chen,[a,b,§] Xiaoting Zeng,[a,§] Abdul Rahim Ferhan,[b] Yuwu Chi,*[,a] Dong-Hwan Kim*[,b] and Guonan Chen[a]

Received (in XXX, XXX) Xth XXXXXXXXX 20XX, Accepted Xth XXXXXXXXX 20XX
DOI: 10.1039/b000000x

A novel permeability gate-based electrochemiluminescent (ECL) aptasensor has been constructed by utilizing target-responsive polyelectrolyte-aptamer film deposited on the solid-state ECL electrode to control the rate of diffusion of a coreactant that triggers the ECL.

Electrochemiluminescence (ECL), as a powerful analytical technique with high sensitivity, has been widely applied in many fields ranging from clinical diagnostics to environmental and food analysis.[1-3] Of the types of ECL, solid-state ECL, that immobilizes ECL luminophore as a sensing substrate at the electrode surface, has attracted considerable attention due to its regenerability, simplicity, portability and low cost,[4,5] and consequently several strategies have been developed.[6] The approaches for the construction of highly sensitive solid-state ECL sensors can be generally classified into four broad categories.[6] First, the inhibitory or enhancing effect of the analytes on the emission of ECL film by means of either energy transfer or electron transfer has been used;[7-9] this strategy usually suffers from limited types of analytes and low selectivity. Second, a strategy to alter the emission of ECL film through the generation or consumption of coreactants via enzymatic reactions were used for the detection of either enzyme substrates or antigens with enzyme-labeled antibodies;[10,11] working with enzymes requires narrow operation parameters (e.g., of pH, temperature, ionic strength) due to the easy loss of bioactivity. Third, steric hindrance from bio-recognition reactions, such as antigen-antibody and aptamer-protein, has enabled the development of signal-off ECL sensing strategy via the insulation of attached biomacromelecules;[12, 13] being restricted to relatively large biomolecule detection and prone to high background. Lastly, ECL resonance energy transfer has been exploited as an efficient sensing strategy by employing overlapped spectra of donor and acceptor;[14,15] this requires suitable pairs of donor and acceptor which are difficult to find. Thus, despite these burgeoning developments, there is a high demand for the development of completely label-free solid-state ECL platform suitable for selective, sensitive, and low cost detection.

Here we report a novel solid-state ECL sensing strategy based on target-responsive permeability gate, as illustrated in Scheme 1. Inspired by the development of stimuli-responsive fluorescent materials[16-18], people have recently begun to pay attention on the construction of stimuli-responsive ECL materials[19]. In this contribution, ECL material combined with polyelectrolyte was employed to develop a stimuli-responsive ECL sensor. Previously, we developed Au-g-C_3N_4 nanohybrids (hereafter referred to as Au-g-C_3N_4) that showed superior ECL efficiency and stability.[20, 21] The Au-g-C_3N_4, as an excellent ECL nano-emitter, was thus employed to modify a glassy carbon electrode (GCE) in the present study. An overlayer of polyelectrolytes thin films containing DNA aptamers on top of the ECL film (see (A) in Scheme 1) were then assembled. DNA aptamers (synthetic nucleic acids that fold into secondary nanostructures capable of binding to a certain target molecule)[22] can maintain their affinity and specificity for the cognate targets when incorporated into the polyelectrolyte layers.[23-25] Adopted from previous reports, the conformational change of the aptamer upon target binding could increase the permeability of the polyelectrolyte film.[23-25] Here, we utilize the thin film of polyelectrolyte-aptamer as gate to control the diffusion of coreactants ($S_2O_8^{2-}$ in present study) that is needed to trigger ECL (B in Scheme 1).The proposed strategy for ECL sensing is unique and advantageous for following reasons. First, although controlling the permeability of polyelectrolyte capsules to allow for the triggered release of a molecular payload has been implicated in drug delivery,[26, 27] this is the first reported attempt to integrate the stimulus-responsive permeability gate into ECL-based sensor. Second, the proposed detection strategy is completely label-free because of the electrostatic assembly of both the probes and targets. Third, high sensitivity can be achieved because of the low background signal resulting from

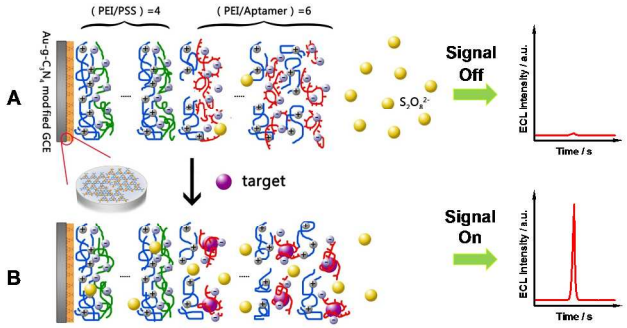

Scheme 1 Schematic principle of the ECL aptasensor with target-responsive permeability gate. Binding of target increases permeability of the polyelectrolyte film and turns on the ECL intensity of Au-g-C_3N_4 film.

ChemComm Accepted Manuscript

effective blockage of coreactants. Fourth, the potential for false signal often induced by quenchers can be eliminated due to the "signal-on" feature of the sensor. Additionally, the sensor is easily fabricated by taking advantages of layer-by-layer (LBL) assembly of polyelectrolytes,[28,29] which is noted for its simplicity and repeatability when fabricating thin polyelectrolyte films with thicknesses in nanometer ranges,[29] and incorporating the aptamers in polyelectrolyte film through LBL assembly greatly simplifies capture probe introduction.

Bisphenol A (BPA) is selected as a model analyte to demonstrate the concept of target-responsive permeability gate based ECL sensor. Detection of BPA, an important raw material that is widely used in plastic industry, such as in the lining of food cans and feeding-bottles, is significant as it is an estrogenic contaminant.[30,31] The BPA aptamer shows high specificity toward BPA at the nano-molar affinity level and folds into a secondary structure upon binding with BPA (Figure S1 in the Supporting Information (SI)).[32]

Au-g-C_3N_4 was synthesized through a conventional solution impregnation method, (see the SI) and anchored on a GCE by directly dropping drops of Au-g-C_3N_4 suspension. The ECL emission characteristic of the Au-g-C_3N_4–$S_2O_8^{2-}$ system is presented in Figure S2. The stable ECL signal can be obtained by adopting the potential window of -1.1 to 0 V (Figure S2A), and the ECL intensity is strongly dependent on the $S_2O_8^{2-}$ concentration in range of 0.1 to 100 mM (Figure S2B). Multilayers of polyelectrolytes were deposited on the negatively charged Au-g-C_3N_4 film. We initiated a layer of polyethylenimine (PEI) (a cationic polyelectrolyte) and subsequently polystyrene sulfonate (PSS) (an anionic polyelectrolyte). After the deposition of multiple layers of PEI/PSS, the BPA aptamer was used as an anionic polyelectrolyte. The electrostatic assembly procedure allows for eliminating a labeling procedure for both the aptamer and the target. The composition of the polyelectrolyte film was optimized to be $(PEI/PSS)_4(PEI/aptamer)_6$ for constructing our sensing platform (Figures S3 and S4). The deposition of $(PEI/PSS)_4(PEI/aptamer)_6$ on the Au-g-C_3N_4 film was further confirmed by scanning electron microscopy (SEM). Figure 1A shows closely packed assembly of Au-g-C_3N_4, representing the excellent film-forming ability of Au-g-C_3N_4. At higher magnification (the inset in Figure 1A), uniformly distributed Au nanoparticles (white spots) on the surface of g-C_3N_4 nanosheets are clearly visible. With deposition of $(PEI/PSS)_4(PEI/aptamer)_6$, the image becomes blurry because of the low conductivity of the deposited polyelectrolyte film (Figure 1B). The higher magnification image of the edge of the polyelectrolyte film (the inset in Figure 1B) confirmed the formation of molecularly smooth polyelectrolyte layers.[33] The atomic force image (AFM) height profile (Figure S5A) shows that the thickness of $(PEI/PSS)_4(PEI/aptamer)_6$ film is about 8 nm.

Subsequently, we evaluated the ECL sensor fabricated with the $(PEI/PSS)_4(PEI/aptamer)_6$ assembled on the Au-g-C_3N_4 film. The strong ECL intensity of Au-g-C_3N_4 film (curve (a) in Figure 1C) was drastically decreased upon the $(PEI/PSS)_4(PEI/aptamer)_6$ film deposition (curve (b) in Figure 1C), suggesting low background of the ECL sensor. The low ECL background might be explained by that the dense coating of the polyelectrolyte film blocks $S_2O_8^{2-}$ from diffusing, the ECL intensity of Au-g-C_3N_4

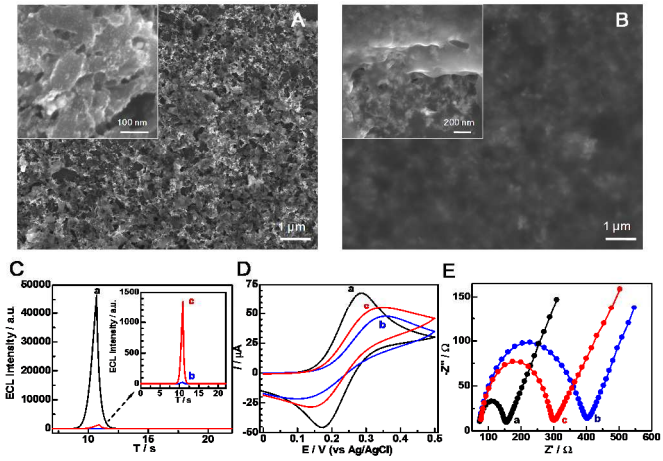

Fig.1 SEM images of Au-g-C_3N_4 film (A) and $[(PEI/PSS)_4(PEI/aptamer)_6]$/Au-g-$C_3N_4$ film (B) on GCE substrates. ECL (C), CV (D) and EIS (E) responses of (a) Au-g-C_3N_4 film /GCE, (b) $[(PEI/PSS)_4(PEI/aptamer)_6]$/Au-g-$C_3N_4$ film /GCE, (c) (b) upon binding of 5 ng mL^{-1} BPA for 40 min. The ECL aptamer sensors were immersed in ECL and EIS test solution for 15 min prior to measurements. ECL was tested in 0.1 M pH 7.4 PBS containing 10 mM $K_2S_2O_8$ at the potential range from 0 to -1.1 V with a scan rate of 100 mV s^{-1}. CV was performed in 0.1 M pH 7.4 PBS containing 10 mM $Fe(CN)_6^{4-}$. EIS was carried out in the solution of 0.1 M KNO_3 containing 20 mM $K_3[Fe(CN)_6]/K_4[Fe(CN)_6]$.

film is strongly dependent on $S_2O_8^{2-}$ concentration, and the electron-donating amines of the innermost PEI layer decrease the hole-transfer efficiency between $S_2O_8^{2-}$ and Au-g-C_3N_4.

To examine the stability of the deposited polyelectrolyte film, the sensor was first immersed in target-free buffer solution. The ECL intensity of the electrode essentially maintains a constant and low value (see curve (a) in Figure S6A), showing no obvious swelling of the film and excellent stability of the sensor. In the presence of target, the spatial arrangement between PEI and BPA aptamer are altered due to the conformational change of the aptamer upon BPA binding, and increases the permeability of the polyelectrolyte film. Therefore, it was expected that the ECL response of the Au-g-C_3N_4 film would recover as the film in the presence of BPA has a higher permeability to the coreactant, $S_2O_8^{2-}$. An enhancement of 64 times in ECL intensity was indeed observed in the presence of 5.0 ng mL^{-1} BPA (curve (c) in Figure 1C). AFM images show that there is no obvious change in film thickness after BPA binding (see Figure S5), ruling out target triggered decomposition of polyelectrolyte film. Cyclic voltammetry (CV) provides an important assessment of ion diffusion pathway variation upon polyelectrolyte deposition and film permeability change. Typically, higher peak currents and a more reversible voltammogram indicate better access to the electrode.[34] As shown in Figure 1D, the CV of Au-g-C_3N_4 film (curve a) upon polyelectrolyte deposition (curve b) become broad and plateau-shaped, suggesting slow diffusion of $Fe(CN)_6^{4-}$ through the polyelectrolyte film. After binding the sensor with 5.0 ng mL^{-1} BPA (curve c), CV shows larger peak currents along with better redox reversibility, indicating variation in polyelectrolyte film structure and thus improvement of the permeability. Additionally, EIS as a complementary technique that allows quantitative determination of kinetic and diffusion

ChemComm Accepted Manuscript

This journal is © The Royal Society of Chemistry [year]

parameters,[35] was employed to further investigate the evolution of ECL and CV response. As shown in Figure 1E, R_{et} of the Au-g-C_3N_4 film modified electrode (curve (a)) increases sharply with the deposition of $(PEI/PSS)_4(PEI/aptamer)_6$ film (curve (b)), and falls back with subsequent BPA binding (curve (c)), which is consistent with the trends shown by ECL (Figure 1C) and CV (Figure 1D). The effect of the length of the polyelectrolyte on the stability and assay performance of the sensor was investigated by replacing the low molecular weight of PEI (~ 10,000 Da) with the high molecular weight of PEI (~ 6,000,000 Da). It is found that the stability of the sensor was not affected by the polyelectrolyte length. However, the sensing response of the sensor constructed by high molecular PEI (ECL enhancement factor of 54 times for 5 ng mL^{-1}) showed slightly lower than that of constructed by low molecular PEI (64 times). This may be attributed to the larger thickness of polyelectrolyte film with high molecular PEI.

Next we optimized the analytical conditions for the sensor. Since several factors, such as BPA binding time and sensor immersion time in ECL test solution, can influence the detection sensitivity of the sensor, we performed a series of experiments to optimize these parameters (Figure S6). After optimization, 40 min and 15 min were respectively selected as target incubation time and sensor immersion time in ECL test solution in the following experiments. After the optimization, the ECL sensor was applied to quantify the concentration of target. BPA standards with concentrations from 0.05 to 500 ng mL^{-1} were tested, with five measurements each in parallel. As shown in Figure 2A, the ECL enhancement factor was proportional to the logarithm concentration of BPA up to 200 ng mL^{-1}, establishing the quantitative detection capability of the ECL sensor. A detection limit of 0.05 ng mL^{-1} BPA was observed based on three times the standard deviation of the blank (as shown in Figure S7). The high detection sensitivity can be explained by the low background of the sensor and the high ECL efficiency of Au-g-C_3N_4 system. The analytical performance of the ECL aptasensor for BPA detection was compared with those of other reported methods (Table S1 in SI). The comparison indicates that the ECL aptasensor is one of the most excellent sensors for BPA detection. To evaluate the selectivity of the ECL sensor, the BPA analogues that may bind to BPA aptamer and metal ions that may affect the ECL property of Au-g-C_3N_4 were applied as latent interferences.[36] 50 ng mL^{-1} analogues and 10 μM metal ions induced negligible ECL enhancement, as shown in Figure 2B. In contrast, BPA at only 5 ng mL^{-1} produced a large ECL enhancement factor. The observed high selectivity can be attributed to the high specificity binding of the BPA aptamer to the BPA molecule, and the effectiveness of polyelectrolyte film to selectively inhibit transport of ions[37]. The reusability was also investigated, and the related results and discussion were provided in SI. The aptasensor could be regenerated by simply unfolding the aptamer in 1.0 M imidazole (Figure S8), showing a good reusability of the sensor. Moreover, the ECL sensor can be universal, as a wide range of aptamers are commercially available for specific targets of interest, and influence of target binding on the permeability of polyelectrolyte-aptamer film is widely observed.[24, 25]

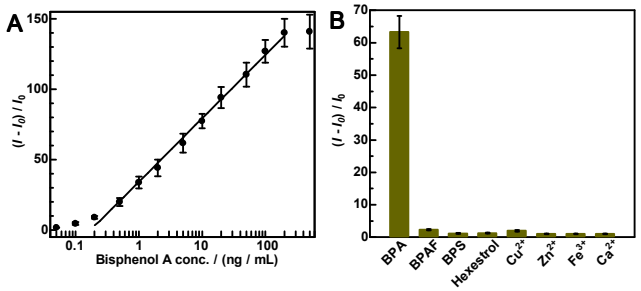

Fig. 2 (A) Dose response of ECL enhancement factor as a function of BPA concentration. (B) Specificity of the ECL aptasensor to BPA (5 ng mL^{-1}) by comparing it to the latent interferents at the 50 ng mL^{-1} level: 2,2-Bis(4-hydroxyphenyl)hexafluoropropane (BPAF), Bis(4-hydroxyphenyl)sulfone (BPS), and hexestrol, and to the metal ions at the 10 μM level. All ECL data was acquired upon immersion the ECL aptamer sensors in different concentration of BPA and various latent interferents for 40 min followed by rinsing with doubly distilled water, and then immersion in ECL test solution for 15 min. All data presented was the average of five parallel assays.

In summary, we have presented a novel solid-state ECL sensing strategy that utilizes stimuli-responsive polyelectrolyte-aptamer thin film to control the diffusion of coreactants that alter the ECL intensity of the solid-state ECL film. The fabrication of the ECL sensor is easy, inexpensive and completely label-free. The sensor shows high sensitivity and great selectivity. Although only BPA detection is demonstrated herein, in view of the wide application of aptamer, the proposed approach can be used for many other small molecule assays. Additionally, advances in the syntheses of new and excellent ECL nanoemitters like C_3N_4 nanosheets, and related solid-state ECL studies have opened a wealth of possibilities for expanding this concept to other ECL coreactant systems. We believe that the sensing platform will prove promising for applications such as high-throughput drug screening and environment monitoring.

This study was financially supported by National Natural Science Foundation of China (21375020), and Specialized Research Fund for the Doctoral Program of Higher Education of China (20133514110001). DHK acknowledges the financial support of the Ministry of Education of Singapore (MOE2012-T2-1-058).

Notes and references

[a] *MOE Key Laboratory of Analysis and Detection Technology for Food Safety, and College of Chemistry, Fuzhou University, Fuzhou, Fujian, 350108, China. Fax: +86-591-22866137; Tel: +86-591-22866137; E-mail: y.w.chi@fzu.edu.cn*

[b] *School of Chemical and Biomedical Engineering, Nanyang Technological University, 70 Nanyang Drive, Singapore 637457, Singapore. E-mail: dhkim@ntu.edu.sg*

§ These authors contributed equally.

† Electronic Supplementary Information (ESI) available: Experimental section, Figures S1-S8, and Table S1. See DOI: 10.1039/b000000x/

1. M. M. Richter, *Chem. Rev.*, 2004, **104**, 3003-3036.
2. W. Miao, *Chem. Rev.*, 2008, **108**, 2506-2553.
3. L. Chen, D. Huang, S. Ren, Y. Chi and G. Chen, *Anal. Chem.*, 2011, **83**, 6862-6867.
4. Z. Guo, Y. Shen, M. Wang, F. Zhao and S. Dong, *Anal. Chem.*, 2003, **76**, 184-191.
5. X. Sun, Y. Du, S. Dong and E. Wang, *Anal. Chem.*, 2005, **77**, 8166-8169.
6. S. Deng and H. Ju, *Analyst*, 2013, **138**, 43-61.

ChemComm Accepted Manuscript

7. C. Z. Wang, Y. F. E, L. Z. Fan, Z. H. Wang, H. B. Liu, Y. L. Li, S. H. Yang and Y. L. Li, *Adv. Mater.*, 2007, **19**, 3677-3681.
8. J. Li, L. Yang, S. Luo, B. Chen, J. Li, H. Lin, Q. Cai and S. Yao, *Anal. Chem.*, 2010, **82**, 7357-7361.
9. G. Zou and H. Ju, *Anal. Chem.*, 2004, **76**, 6871-6876.
10. X.-F. Wang, Y. Zhou, J.-J. Xu and H.-Y. Chen, *Adv. Funct. Mater.*, 2009, **19**, 1444-1450.
11. S. Deng, J. Lei, Y. Huang, X. Yao, L. Ding and H. Ju, *Chem. Commun.*, 2012, **48**, 9159-9161.
12. L.-L. Li, K.-P. Liu, G.-H. Yang, C.-M. Wang, J.-R. Zhang and J.-J. Zhu, *Adv. Funct. Mater.*, 2011, **21**, 869-878.
13. G. Jie, J. Zhang, D. Wang, C. Cheng, H.-Y. Chen and J.-J. Zhu, *Anal. Chem.*, 2008, **80**, 4033-4039.
14. Y. Shan, J.-J. Xu and H.-Y. Chen, *Chem. Commun.*, 2009, 905-907.
15. J. Wang, Y. Shan, W.-W. Zhao, J.-J. Xu and H.-Y. Chen, *Anal. Chem.*, 2011, **83**, 4004-4011.
16. C. Li, T. Wu, C. Hong, G. Zhang and S. Liu, *Angew. Chem., Int. Ed.*, 2012, **124**, 470-474.
17. S. Lee, J. H. Ryu, K. Park, A. Lee, S.-Y. Lee, I.-C. Youn, C.-H. Ahn, S. M. Yoon, S.-J. Myung, D. H. Moon, X. Chen, K. Choi, I. C. Kwon and K. Kim, *Nano Lett.*, 2009, **9**, 4412-4416.
18. C. H. Li and S. Y. Liu, *Chem. Commun.*, 2012, **48**, 3262-3278.
19. F. Pinaud, L. Russo, S. Pinet, I. Gosse, V. Ravaine and N. Sojic, *J. Am. Chem. Soc.*, 2013, **135**, 5517-5520.
20. L. Chen, X. Zeng, P. Si, Y. Chen, Y. Chi, D.-H. Kim and G. Chen, *Anal. Chem.*, 2014, **86**, 4188-4195.
21. L. Chen, D. Huang, S. Ren, T. Dong, Y. Chi and G. Chen, *Nanoscale*, 2013, **5**, 225-230.
22. D. H. J. Bunka and P. G. Stockley, *Nat. Rev. Microbiol.*, 2006, **4**, 588-596.
23. Y. Sultan, R. Walsh, C. Monreal and M. C. DeRosa, *Biomacromolecules*, 2009, **10**, 1149-1154.
24. Y. Sultan and M. C. DeRosa, *Small*, 2011, **7**, 1219-1226.
25. B. Malile and J. I. L. Chen, *J. Am. Chem. Soc.*, 2013, **135**, 16042-16045.
26. Y. Zhu, J. Shi, W. Shen, X. Dong, J. Feng, M. Ruan and Y. Li, *Angew. Chem., Int. Ed.*, 2005, **117**, 5213-5217.
27. B. G. De Geest, N. N. Sanders, G. B. Sukhorukov, J. Demeester and S. C. De Smedt, *Chem. Soc. Rev.*, 2007, **36**, 636-649.
28. G. Decher, J. D. Hong and J. Schmitt, *Thin Solid Films*, 1992, **210–211, Part 2**, 831-835.
29. G. Decher, *Science*, 1997, **277**, 1232-1237.
30. K. L. Howdeshell, A. K. Hotchkiss, K. A. Thayer, J. G. Vandenbergh and F. S. vom Saal, *Nature*, 1999, **401**, 763-764.
31. C. Liao and K. Kannan, *Environ. Sci. Technol.*, 2011, **45**, 6761-6768.
32. M. Jo, J. Y. Ahn, J. Lee, S. Lee, S. W. Hong, J. W. Yoo, J. Kang, P. Dua, D. K. Lee, S. Hong and S. Kim, *Oligonucleotides*, 2011, **21**, 85-91.
33. Y. Lvov, K. Ariga, I. Ichinose and T. Kunitake, *J. Am. Chem. Soc.*, 1995, **117**, 6117-6123.
34. J. J. Harris and M. L. Bruening, *Langmuir*, 2000, **16**, 2006-2013.
35. A. J. Bard and L. R. Faulkner, *Electrochemical Methods: Fundamentals and Applications*, Wiley, 2000.
36. C. Cheng, Y. Huang, X. Tian, B. Zheng, Y. Li, H. Yuan, D. Xiao, S. Xie and M. M. F. Choi, *Anal. Chem.*, 2012, **84**, 4754-4759.
37. L. Krasemann and B. Tieke, *Langmuir*, 1999, **16**, 287-290.

ChemComm Accepted Manuscript

This journal is © The Royal Society of Chemistry [year]